Fermi-Edge Singularities in the Mesoscopic X-Ray Edge Problem

Martina Hentschel,[1] Denis Ullmo,[1, 2] and Harold U. Baranger[1]

[1] *Department of Physics, Duke University, Box 90305, Durham, NC 27708-0305*
[2] *Laboratoire de Physique Théorique et Modèles Statistiques (LPTMS), 91405 Orsay Cedex, France*
(Dated: February 2, 2008)

We study the x-ray edge problem for a chaotic quantum dot or nanoparticle displaying mesoscopic fluctuations. In the bulk, x-ray physics is known to produce Fermi edge singularities – deviations from the naively expected photoabsorption cross section in the form of a peaked or rounded edge. For a coherent system with chaotic dynamics, we find substantial changes; in particular, a photoabsorption cross section showing a rounded edge in the bulk will change to a slightly peaked edge on average as the system size is reduced to a mesoscopic (coherent) scale.

The x-ray edge problem for metals refers to a singularity at threshold in the photoabsorption spectra associated with the excitation of a core electron to the conduction band by an x ray. The singularity takes the form of a peaked or rounded edege and was studied intensively over the last four decades using different methods [1]. The sustained attention devoted to this problem developed because the basic phyiscs originally studied for x-ray absorption recurs in many other contexts. Recently, photoabsorption in semiconductor quantum wells [2] and electrical conduction through localized states [3] have been particularly active areas of Fermi edge research. Motivated by the growing interest in nanoscale systems like quantum dots or nanoparticles [4, 5, 6], we address Fermi edge physics for such confined geometries, assuming generic chaotic dynamics of the electrons.

For bulk metals or degenerately doped semiconductors, the photoabsorption cross section $A(\omega)$ near the threshold energy $\omega_{\rm th}$ involves two competing effects, Mahan's enhancement and Anderson's orthogonality catastrophe (AOC). Its form is [1]

$$A(\omega) \propto (\omega - \omega_{\rm th})^{-2\left(|\delta_{l_0}|/\pi\right)+\sum_l 2(2l+1)(\delta_l/\pi)^2} . \quad (1)$$

Here δ_l is the partial-wave phase shift at the Fermi energy associated with the core hole potential $\hat{V}_c$ for orbital channel l; l_0 is the optically excited channel. The phase shifts obey the Friedel sum rule $Z = \sum_l 2(2l+1)\delta_l/\pi$ with $Z = -1$ here. AOC [7] reduces the overlap between ground states before and after $\hat{V}_c$ is applied, leading to a rounded edge. On the other hand, the sudden presence of a charge associated with the missing core electron entails a many body response that enhances the threshold cross section, resulting in a peaked edge. Whereas all l channels are sensitive to $\hat{V}_c$ and so contribute to AOC (second term in the exponent), only the optically excited l_0 experiences the many-body interaction (first term).

The many-body enhancement depends, via the dipole selection rule, on the symmetry of both the core electron and local conduction electron wavefunctions. We will assume the latter to be of s-type, and distinguish between core electrons with s-symmetry (K-shell) and p-symmetry (L$_{2,3}$-shell) [8], referring to the photoabsorption threshold as a K- or L-edge, respectively. Furthermore, we take the core hole potential to be spherically symmetric: $\delta_l = 0$ for $l \neq 0$. The Friedel sum rule then implies $\delta_0 = -\pi/2$, so that either a rounded K-edge ($l_0 = 1$, photoabsorption dominated by AOC) or a peaked L-edge ($l_0 = 0$) is found. For mesoscopic systems, in addition to $\delta_0 \approx -\pi/2$, we shall consider smaller values for situations where other charges (e.g. on nearby gates in a semiconductor heterostructure) help to screen the core hole.

Compared to bulk metals, some characteristics intrinsic to nanoscale objects will significantly alter the x-ray edge properties. First, the fact that both the number of electrons and the total number of levels are finite will lead to an incomplete AOC and many-body enhancement. Furthermore, the lack of rotational symmetry eliminates independent orbital momentum channels. Finally, mesoscopic fluctuations will affect both energy levels and wavefunctions. In tackling these issues, the key ingredient is the joint statistics of the electronic properties before and after the core hole excitation [9].

The influence of these effects on the average and fluctuations of the Anderson overlap was modeled using parametric random matrices [10] and for disordered systems [11]. These studies mainly addressed the regime where the added potential can be treated perturbatively, as, for instance, for scrambling phenomena in Coulomb blockade experiments. Here, we study first AOC and then absorption spectra near threshold for a model corresponding to the x-ray edge problem. In this case the perturbing potential $\hat{V}_c$ associated with the core hole has a very short range, but on the other hand strong perturbations are physically relevant. Possible experimental realizations are briefly discussed in the conclusion.

We model the conduction electrons of our mesoscopic system in the absence of the core hole by the non-interacting $\hat{H}_0 = \sum_{i,\sigma} \epsilon_i c_{i,\sigma}^\dagger c_{i,\sigma}$, where $c_{i,\sigma}^\dagger$ creates a particle with spin $\sigma = \pm$ in the orbital $\varphi_i(\mathbf{r})$ ($i = 0, \ldots, N-1$). We furthermore assume that the perturb-

ing potential is a contact potential $\hat{V}_c = \mathcal{V}v_c|\mathbf{r}_c\rangle\langle\mathbf{r}_c|$, with $\mathbf{r}_c$ the location of the core hole and $\mathcal{V}$ the volume of the system. The diagonal form of the perturbed Hamiltonian is $\hat{H} = \hat{H}_0 + \hat{V}_c = \sum_{i,\sigma} \lambda_i \tilde{c}^\dagger_{i,\sigma} \tilde{c}_{i,\sigma}$, where $\tilde{c}^\dagger_{i,\sigma}$ creates a particle in the perturbed orbital $\psi_i(\mathbf{r})$. For the Fermi energy in the middle of the conduction band, δ_0, v_c and the mean level spacing d are related through $\delta_0 = \arctan(\pi v_c/d)$ [1] (δ_0 is negative since the core potential is attractive).

A remarkable property of a rank one perturbation such as a contact potential is that all the quantities of interest for the x-ray edge problem can be either expressed in terms of the $\{\epsilon\}$ and $\{\lambda\}$ or taken as independent random variables. For instance, ignoring for now the spin variable, the overlap between the many body ground states with M particles Φ_0 and Ψ_0 of $\hat{H}_0$ and $\hat{H}$ is [1]

$$|\Delta|^2 = |\langle\Psi_0|\Phi_0\rangle|^2 = \prod_{i=0}^{M-1}\prod_{j=M}^{N-1} \frac{(\lambda_j - \epsilon_i)(\epsilon_j - \lambda_i)}{(\lambda_j - \lambda_i)(\epsilon_j - \epsilon_i)} . \quad (2)$$

For chaotic mesoscopic systems, we may assume that the unperturbed energy levels follow random matrix theory fluctuations and the wave function intensities are Porter-Thomas distributed (in particular at $\mathbf{r}_c$) [12]. Under these hypotheses, the joint probability distribution $P(\{\epsilon\}, \{\lambda\})$ was derived by Aleiner and Matveev [9] (see [13] for a generalization to the non-rank-one case):

$$P(\{\epsilon\}, \{\lambda\}) \propto \frac{\prod_{i>j}(\epsilon_i - \epsilon_j)(\lambda_i - \lambda_j)}{\prod_{i,j} |\epsilon_i - \lambda_j|^{1-\beta/2}} e^{-\frac{\beta}{2}\sum_i (\lambda_i - \epsilon_i)/v_i} \quad (3)$$

with the constraint $\epsilon_{i-1} \leq \lambda_i \leq \epsilon_i$. Here $\beta = 1$ (circular orthogonal ensemble, COE) or $\beta = 2$ (circular unitary ensemble, CUE) for the time reversal symmetric or asymmetric case, respectively. In the middle of the band $v_i = v_c$. In our case, it turns out to be necessary to include boundary effects [14], which modify the phase shifts away from the band center. This can be done simply by using a variable v_i given by

$$\frac{1}{v_i} = \frac{1}{v_c} + \frac{1}{d}\ln\frac{N - 0.5 - i}{i + 0.5} . \quad (4)$$

for $i \in [0, (N-1)/2]$, and the analogous form for $i \in [(N-1)/2, N-1]$. In addition, at perturbation strengths $|v_c| \gtrsim 0.5d$, the lowest perturbed level λ_0 requires special treatment as its mean shift $\langle\lambda_0 - \epsilon_0\rangle = -Nd/[\exp(|d/v_c|) - 1]$ becomes large. This gives rise to a second band in the x-ray spectra [1] that we do not discuss here.

Using a Metropolis algorithm, we can therefore generate ensembles of $(\{\epsilon\}, \{\lambda\})$ with the proper joint distribution, Eq. (3), and using Eq. (2) build the distribution of overlap for any value of the parameters M, N, v_c, and β. To quantify the role of fluctuations, we define for reasons of comparison the special case of equidistant unperturbed levels $\{\epsilon\}$, and will refer to it as the uniform or "bulklike" case with overlap $|\Delta_b|^2$ ($\propto N^{-\delta_F^2/\pi^2}$).

Results of such a simulation are displayed in Figs. 1 and 2. The probability distributions of the overlap $P(|\Delta|^2)$ shown in Fig. 1(a) differ considerably even though the phase shift at the Fermi energy, $\delta_F \equiv \arctan(\pi v_{i=M}/d)$, is similar. In fact, as expected, we find that both $P(|\Delta|^2)$ and the bulklike result $|\Delta_b|^2$ depend independently on N, M, and δ_F. However, performing a scaling by $|\Delta_b|^2$, see Fig. 1(b), causes all curves with the same δ_F to collapse. *Thus, the fluctuations of the overlap depend only on the value of the phase shift at the Fermi energy, δ_F.*

The small $|\Delta|^2$ part of $P(|\Delta|^2)$ can be accurately reproduced, as in the cases studied in Refs. [10, 11], by incorporating the fluctuations of only the levels closest to the Fermi energy. For instance, we may multiply $|\Delta_b|^2$ by the fluctuating factor $[1/(1 - \delta_F/\pi)](\lambda_{M+1} - \epsilon_M)/(\lambda_{M+1} - \lambda_M)$, which we call the "range-1" approximation. The resulting distribution (Fig. 2) is already similar to the exact one. We found an analytical result for this approximation for both the COE and CUE cases by treating two fluctuating levels and reducing the remaining ones to a single Gaussian variable [14]; it is seen to coincide with the range-1 result over the whole range of $|\Delta|^2$.

We can similarly define "range-n" approximations which include the fluctuations of n levels on each side of the Fermi energy. The range-2 approximation matches the exact one for large perturbation strengths (Fig. 2),
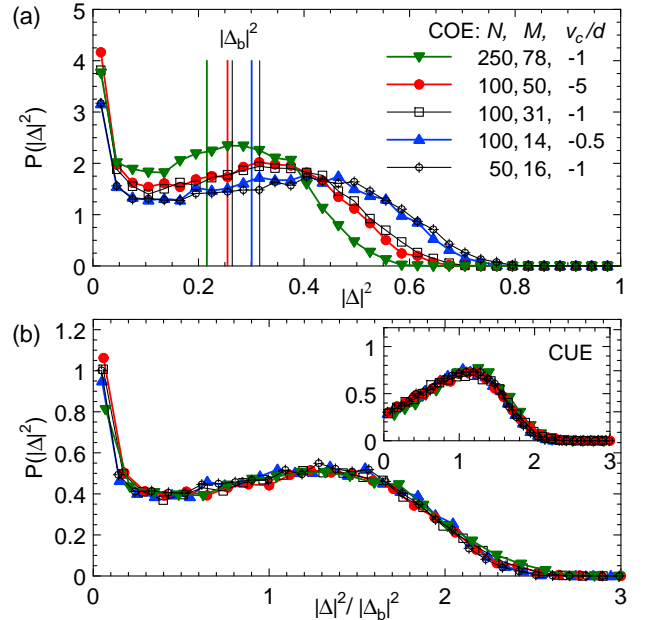

FIG. 1: (Color online) Probability distribution $P(|\Delta|^2)$ of the overlap $|\Delta|^2$ for different parameter sets $\{N, M, -v_c/d\}$. (a) Although all $\delta_F \approx -\pi/2$, the $P(|\Delta|^2)$ are visibly different as a result of different bulklike overlaps $|\Delta_b|^2$ (increasing with the legend entries, COE case). (b) The curves coincide when scaled with $|\Delta_b|^2$. The inset shows the CUE result with a noticeably different $P(|\Delta|^2)$ distribution for small $|\Delta|^2$ originating from the different wavefunction statistics.
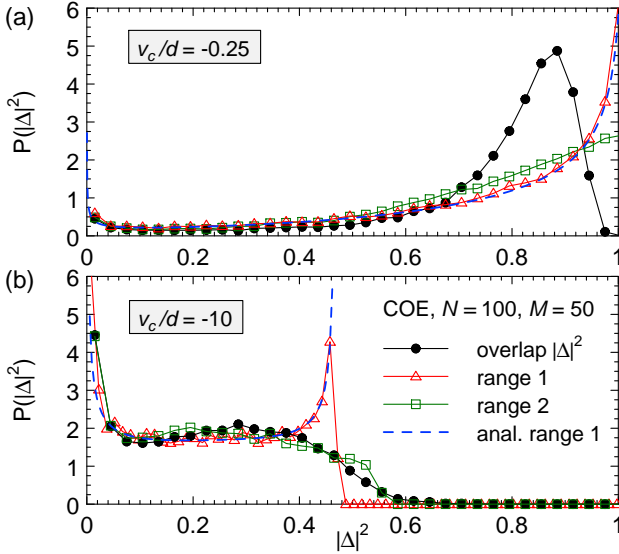
FIG. 2: (Color online) Exact and approximate probability distributions of the overlap for (a) weak ($v_c/d = -0.25$) and (b) strong ($v_c/d = -10$) perturbation (COE, $N = 100, M = 50$). The exact $P(|\Delta|^2)$ is increasingly well reproduced by the range-1 and range-2 approximation, indicating that the fluctuations originate from levels around the Fermi energy. The dashed line denotes the range-1 analytical result.

but does not improve significantly on the range-1 approximation for weak perturbations. We have checked, however, that even in this case, it is sufficient to treat a few levels around E_F exactly to obtain the correct $P(|\Delta|^2)$. This retrospectively justifies our use of a full random matrix to model our chaotic systems – the levels beyond the Thouless energy, where such a model does not apply [15], do not affect the overlap distribution.

Turning now to the absorption spectra, we limit our discussion to the K-edge (s-symmetry of the core electron wavefunction) and approach the mesoscopic x-ray edge problem using Fermi's golden rule [1],

$$A(\omega) = 2\pi\hbar^{-1} \sum_f |\langle \Psi_f|\hat{D}|\Phi_0^c\rangle|^2 \delta(E_f - E_0^c - \omega), \quad (5)$$

where the sum is taken over all perturbed final states Ψ_f connected to the unperturbed groundstate $\Phi_0^c = \prod_{\sigma=\pm} \prod_{j=0}^{M-1} c_{j,\sigma}^\dagger|c\rangle$ by the dipole operator $\hat{D}$. ($|c\rangle = c_c^\dagger|0\rangle$ is the empty band plus a core electron of spin $\sigma = +$.) We are interested in processes involving the core hole; thus, the dipole operator can be written as $\hat{D} = \text{const} \sum_{j=0}^N \left(w_j \tilde{c}_{j,+}^\dagger c_c + h.c. \right)$. Since we assume the core electron wavefunction and the local part of the conduction electron wavefunction are both s wave, w_j is related to the derivative of the perturbed orbital ψ_j in the direction $\vec{e}$ of the polarization of the x ray through $w_j = \vec{e} \cdot \nabla \psi_j(\mathbf{r}_c)$.

First consider conduction electrons with the same spin as the excited core electron, and assume $\omega = \omega_{th}$ so that

the only possible final state is $\Psi_{f^0}^+ = \prod_{j=0}^M \tilde{c}_{j,+}^\dagger$. Without a perturbing potential, the only contribution is the direct process $w_M \tilde{c}_{M,+}^\dagger c_0$. In the presence of a perturbation, however, the new and old orbitals are not identical, and terms with $j < M$ (called replacement processes) also contribute coherently, giving [1]

$$|\langle \Psi_{f^0}|\hat{D}|\Phi_0^c\rangle|^2 \propto |w_M\Delta|^2 \left| 1 - \sum_{i=0}^{M-1} \frac{w_i \Delta_{\bar{i},M}}{w_M \Delta} \right|^2 \quad (6)$$

where $\Delta_{\bar{i},M}$ is defined by generalizing Eq. (2) with level $i \, (< M)$ replaced by M. Since for chaotic systems the derivative of the wavefunction, $\mathcal{V}k^{-2} \times |\nabla_{\vec{e}}\psi_j|^2$, is known to have Porter-Thomas fluctuations uncorrelated with the wavefunction itself [16], we can proceed as for the overlap to construct the distribution of $|\langle \Psi_{f^0}|\hat{D}|\Phi_0^c\rangle|^2$.

Away from threshold, part of the x-ray energy can excite additional electrons above the Fermi energy in so-called shake-up processes. Their contribution is a straightforward generalization of Eq. (6). The number of these processes grows in principle exponentially with the energy of the x ray. However, it remains finite even for large $\omega - \omega_{th}$ (and not very large for the values of M and N here) if one considers only shake-up processes that contribute significantly to absorption. Electrons with spin opposite to the excited core electron (spectator spin) affect the absorption only through AOC.

Mesoscopic fluctuations occur in both the photoabsorption $A(\omega)$ and the excess energy $\omega - \omega_{th}$; the former arise from fluctuations in the dipole matrix elements and all energy levels, the latter from the levels above the Fermi energy. Here we limit ourselves to studying the average values of $A(\omega)$; fluctuations will be discussed elsewhere [14]. We give $\langle A(\omega)\rangle$ at the average excitation energy for a given final state, and measure all energies in mean level spacings d from the threshold ω_{th} at which the core electron is excited to the perturbed level λ_M just above the Fermi energy. The normalized results are in Fig. 3(a). The potential strength $v_c = -10d$ is chosen so that the Friedel sum rule is fulfilled ($\delta_0 \approx -\pi/2$, $\delta_{l>0} = 0$). Shown are the spectra for the two spin types and the total result. We find a peaked edge for the optically active spin sector as well as for the full spin result (obtained after convolution with the spectator spin) [17].

It is interesting to compare the chaotic case to the bulk-like situation (equidistant $\{\epsilon\}$ and constant dipole matrix elements). Here, however, since each orbital channel acts "independently", one needs to specify whether the optically active channel is the one affected by the perturbation. As mentioned before, we have assumed s-type local symmetries, corresponding to a K-edge ($l_0 = 1$, $\delta_{l>0} = 0$, $\delta_{l=0} \approx -\pi/2$). Since then only AOC plays a role, the bulklike situation gives a *rounded* edge; in contrast, a *peaked* edge is found in the mesoscopic (chaotic) case [Fig. 3(b)]. This striking difference is an effect of the coherent confinement in the chaotic system, in which
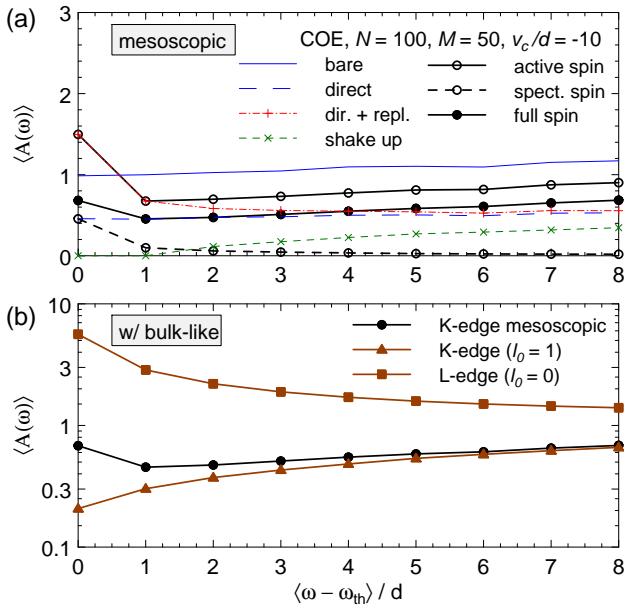
FIG. 3: (Color online) X-ray photoabsorption spectra for (a) the mesoscopic (chaotic) and (b) the bulklike (non-fluctuating) case in terms of averaged cross sections (COE, $N = 100, M = 50, v_c/d = -10$). (a) The mesoscopic spectrum (filled circles) shows a (slightly) peaked edge. Open circles indicate the individual spin contributions for the optically active (full line) and spectator (dashed line) spins. The former arises as the sum of direct and replacement (dashed-dotted), as well as shake-up (dashed, crosses), processes. For comparison we give the bare spectrum (thin line) without either AOC or many-body effects, and the result with AOC only (direct process, thin dashed line). (b) Comparison of the peaked mesoscopic spectrum (circles) to the bulklike results for the same optical channel (triangles, $l_0 = 1$) that shows a rounded K-edge. The mesoscopic peak is, however, less pronounced than the bulklike L-edge (squares, $l_0 = 0$).

coupling is to the derivative of the wave function and so independent of the wave function itself.

This peak is less pronounced, however, than that for the bulklike L-edge case ($l_0 = 0$, so the optically excited and perturbed channels coincide). Because the dipole matrix elements w_i fluctuate in sign and magnitude in the mesoscopic case, the coherence of the replacement processes is less effective. Another difference between these two cases concerns their N-dependence: whereas the peak sharpens with increasing N for the bulklike case, it diminishes with N in the chaotic situation.

The basic physics we study – Fermi edge singularities due to a localized (rank one) perturbation acting on a finite number of chaotic electrons via Fermi golden rule (dipole) matrix elements – is very general and allows a multitude of experimental realizations [2, 3, 14]. The technical requirements for a direct implementation of mesoscopic x-ray absorption considered here using metal-lic nanoparticles may be met within a few years. Another realization would be a double quantum dot with a tiny constriction [18]. Feasible with currently standard semiconductor nanotechnology is an experiment based on a quantum dot array where the role of the core electron is taken by a localized electron bound to a (suitable) impurity level in the band gap. The excitation energy is provided by a micrometer laser that allows energy resolution well below a mean level spacing. Our results predict a (slightly) peaked K-edge in the average photoabsorption that becomes rounded for a bulk two-dimensional electron gas.

[1] For a review and further references, see K. Ohtaka and Y. Tanabe, Rev. Mod. Phys. **62**, 929 (1990); Y. Chen and J. Kroha, Phys. Rev. B, **46**, 1332 (1992).
[2] See, e.g., M. S. Skolnik, *et al.*, Phys. Rev. Lett. **58**, 2130 (1987); I. E. Perakis and T. V. Shahbazyan, Surf. Sci. Rep. **40**, 1 (2000); and references therein.
[3] See, e.g., I. Hapke-Wurst, *et al.*, Phys. Rev. B **62**, 12621 (2000) and references therein.
[4] L. L. Sohn, G. Schön, and L. P. Kouwenhowen, *Mesoscopic Electron Transport* (Kluwer, Dordrecht, 1997).
[5] Y. Alhassid, Rev. Mod. Phys. **72**, 895 (2000).
[6] J. von Delft and D. C. Ralph, Phys. Rep. **345**, 62 (2001).
[7] P. W. Anderson, Phys. Rev. Lett. **18**, 1049 (1967).
[8] P. H. Citrin, G. K. Wertheim, and M. Schlüter, Phys. Rev. B **20**, 3067 (1979).
[9] I. L. Aleiner and K. A. Matveev, Phys. Rev. Lett. **80**, 814 (1998).
[10] R. O. Vallejos, C. H. Lewenkopf, and Y. Gefen, Phys. Rev. B **65**, 085309 (2002).
[11] Y. Gefen, R. Berkovits, I. V. Lerner, and B. L. Altshuler, Phys. Rev. B **65**, 081106(R) (2002).
[12] O. Bohigas, in *Chaos and Quantum Physics*, edited by M.-J. Giannoni, A. Voros, and J. Zinn-Justin (North Holland, 1991), pp. 87-199.
[13] I. E. Smolyarenko, F. M. Marchetti, and B. D. Simons, Phys. Rev. Lett. **88**, 256808 (2002).
[14] M. Hentschel, D. Ullmo, and H. U. Baranger, in preparation.
[15] I. L. Aleiner, P. W. Brouwer, and L. I. Glazman, Phys. Rep. **358**, 309 (2002).
[16] V. N. Prigodin, N. Taniguchi, A. Kudrolli, V. Kidambi, and S. Sridhar, Phys. Rev. Lett. **75**, 2392 (1995).
[17] Whereas the averaged photoabsorption has a peaked edge, individual spectra may show "zig-zagging" points.
[18] D. A. Abanin and L. S. Levitov, Phys. Rev. Lett.**93**, 126802 (2004).